Efficient Implementation of Equation-of-Motion Coupled-Cluster Singles and Doubles Method with the Density-Fitting Approximation: An Enhanced Algorithm for the Particle–Particle Ladder Term

Aslı Ünal and Uğur Bozkaya*

Read Online

ACCESS | Metrics & More | Article Recommendations | Supporting Information

ABSTRACT: An efficient implementation of the density-fitted equation-of-motion coupled-cluster singles and doubles (DF-EOM-CCSD) method is presented with an enhanced algorithm for the particle–particle ladder (PPL) term, which is the most expensive part of EOM-CCSD computations. To further improve the evaluation of the PPL term, a hybrid density-fitting/Cholesky decomposition (DF/CD) algorithm is also introduced. In the hybrid DF/CD approach, four virtual index integrals are constructed on-the-fly from the DF factors; then, their partial Cholesky decomposition is simultaneously performed. The computational cost of the DF-EOM-CCSD method for excitation energies is compared with that of the resolution of the identity EOM-CCSD (RI-EOM-CCSD) (from the Q-CHEM 5.3 package). Our results demonstrate that DF-EOM-CCSD excitation energies are significantly accelerated compared to RI-EOM-CCSD. There is more than a 2-fold

reduction for the C_8H_{18} molecule in the cc-pVTZ basis set with the restricted Hartree-Fock (RHF) reference. This cost savings results from the efficient evaluation of the PPL term. In the RHF based DF-EOM-CCSD method, the number of flops (NOF) is $1/4O^2V^4$, while that of RI-EOM-CCSD was reported (Epifanovsky et al. *J. Chem. Phys.* **2013**, *139*, 134105) to be $5/8O^2V^4$ for the PPL contraction term. Further, the NOF of *VVVV*-type integral transformation is $1/2V^4N_{aux}$ in our case, while it appears to be V^4N_{aux} for RI-EOM-CCSD. Hence, our implementation is 2.5 and 2.0 times more efficient compared to RI-EOM-CCSD for these expensive terms. For the unrestricted Hartree-Fock (UHF) reference, our implementation maintains its enhanced performance and provides a 1.8-fold reduction in the computational time compared to RI-EOM-CCSD for the C_7H_{16} molecule. Our results indicate that our DF-EOM-CCSD implementation is 1.7 and 1.4 times more efficient compared with RI-EOM-CCSD for average computational cost per EOM-CCSD iteration. Moreover, our results show that the new hybrid DF/CD approach improves upon the DF algorithm, especially for large molecular systems. Overall, we conclude that the new hybrid DF/CD PPL algorithm is very promising for large-sized chemical systems.
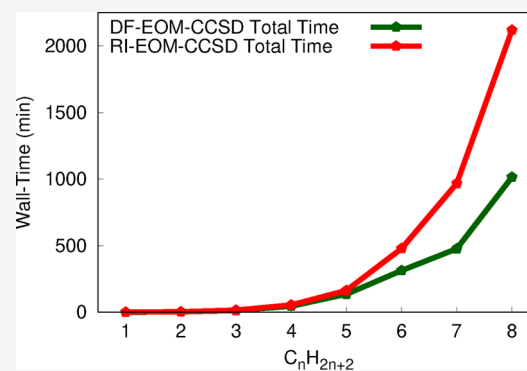
1. INTRODUCTION

It is well-known that coupled-cluster (CC) methods provide accurate results for molecular properties for most chemical systems near equilibrium geometries.[1−13] For example, the coupled-cluster singles and doubles (CCSD) method[14] provides quite accurate results for most molecular systems at equilibrium geometries. The addition of a perturbative triples excitations correction [CCSD(T)][10,11,15] further enhances CCSD and yields very accurate results for a broad range of molecular systems.[12,16−25] However, high computational costs of common CC methods, such as $O(N^6)$ and $O(N^7)$ for CCSD and CCSD(T) (where N is the number of basis functions), limits their applications to relatively small-sized chemical systems.

Accurate computations of excitation energies (EEs) is one of the most challenging problems in modern quantum chemistry. Equation-of-motion CC (EOM-CC) methods provide accurate

results for excited-state properties for a broad range of chemical systems.[26−44] The accuracy of the EOM approach based on the CCSD model (EOM-CCSD) has been reported to be 0.1−0.2 eV.[28,31] However, as in the case of the ground-state CC methods, the computational cost and disk/memory requirements for the EOM-CC methods scale steeply with the system size.

Tensor decomposition techniques for electron repulsion integrals (ERIs) have been of significant interest in modern

computational chemistry.[45−70] Density fitting (DF) is one of the most popular ERI decomposition techniques.[45−52,59−70] In the DF approach, the ERI tensor of rank-4 is expanded in terms of rank-3 tensors. Another common ERI factorization approach is the partial Cholesky decomposition (CD).[55−60,63,64] The DF and CD techniques are very useful to reduce the cost of integral transformations and the storage requirements for the ERI tensor.

In this research, a new implementation of the density-fitted EOM-CCSD method is presented with an enhanced algorithm for the particle−particle ladder (PPL) term, which is the most expensive term. The equations presented have been implemented in a new computer code by the present authors and added to the MacroQC package.[71] The computational time of our DF-EOM-CCSD implementation is compared with that of the Q-chem 5.3 software.[72] The DF-EOM-CCSD method is applied to a test set for excitation energies.

2. CCSD ENERGY AND AMPLITUDE EQUATIONS

At first, we would like to note that all equations reported in this study are in the spin−orbital formalism. The spin-free version of our equations for the restricted closed-shell systems are provided in the Supporting Information. The unrestricted version of the formulas can be readily obtained from the spin−orbital equations.

The correlation energy for the CCSD method can be expressed as follows

$$\Delta E = \langle 0|e^{-\hat{T}}\hat{H}_N e^{\hat{T}}|0\rangle \tag{1}$$

where $\hat{H}_N$ is the normal-ordered Hamiltonian operator,[4,73] $|0\rangle$ is the Hartree−Fock (HF) determinant, and $\hat{T}$ is the sum of single- and double-excitation operators $\hat{T} = \hat{T}_1 + \hat{T}_2$:

$$\hat{T}_1 = \sum_i^{occ} \sum_a^{vir} t_i^a \hat{a}^\dagger \hat{i} \tag{2}$$

$$\hat{T}_2 = \frac{1}{4} \sum_{i,j}^{occ} \sum_{a,b}^{vir} t_{ij}^{ab} \hat{a}^\dagger \hat{b}^\dagger \hat{j} \hat{i} \tag{3}$$

where $\hat{a}^\dagger$ and $\hat{i}$ are the creation and annihilation operators and t_i^a and t_{ij}^{ab} are the single and double excitation amplitudes, respectively.

t_i^a and t_{ij}^{ab} can be obtained from the following equations:

$$\langle \Phi_i^a |e^{-\hat{T}}\hat{H}_N e^{\hat{T}}|0\rangle = 0 \tag{4}$$

$$\langle \Phi_{ij}^{ab} |e^{-\hat{T}}\hat{H}_N e^{\hat{T}}|0\rangle = 0 \tag{5}$$

where Φ_i^a and Φ_{ij}^{ab} are singly and doubly excited Slater determinants, respectively. For explicit equations of our CCSD implementation, one may refer to our previous studies.[65−67]

3. THE EOM-CCSD MODEL

In the EOM-CCSD framework, the target excited-state wave functions are written as follows:

$$|\Psi_R\rangle = \hat{R}e^{\hat{T}}|0\rangle \tag{6}$$

$$\langle \Psi_L| = \langle 0|e^{-\hat{T}}\hat{L} \tag{7}$$

where $\hat{R}$ and $\hat{L}$ are linear excitation and de-excitation operators, respectively. For EOM-CCSD, $\hat{R} = \hat{R}_1 + \hat{R}_2$:

$$\hat{R}_1 = \sum_{ia} r_i^a \{\hat{a}^\dagger \hat{i}\} \tag{8}$$

$$\hat{R}_2 = \frac{1}{4} \sum_{ijab} r_{ij}^{ab} \{\hat{a}^\dagger \hat{b}^\dagger \hat{j} \hat{i}\} \tag{9}$$

where r_i^a and r_{ij}^{ab} are the single and double excitation amplitudes, respectively, and the notation $\{\hat{a}^\dagger...\hat{i}\}$ denotes a string of normal-ordered operators with respect to the Fermi vacuum.

For the ground state, we have the following Schrödinger equation:

$$\hat{H}e^{\hat{T}}|0\rangle = Ee^{\hat{T}}|0\rangle \tag{10}$$

Hence, by multiplying eq 10 by $e^{-\hat{T}}$, we obtain

$$\bar{H}|0\rangle = E|0\rangle \tag{11}$$

where $\bar{H} = e^{-\hat{T}}\hat{H}e^{\hat{T}}$.

Further, the normal ordered $\bar{H}$ can be written as follows:

$$\bar{H} = \hat{\mathcal{H}} + \langle 0|\hat{H}|0\rangle \tag{12}$$

Hence, we define:

$$\hat{\mathcal{H}} = e^{-\hat{T}}\hat{H}_N e^{\hat{T}} = (\hat{H}_N e^{\hat{T}})_c \tag{13}$$

where subscript c means that only connected diagrams should be included. Therefore, we may rewrite eq 11 as follows

$$\hat{\mathcal{H}}|0\rangle = \Delta E|0\rangle \tag{14}$$

where ΔE is the ground-state CC correlation energy.

The excited-state eigenvalue equation can be written as follows:

$$\hat{\mathcal{H}}\hat{R}|0\rangle = \Delta E_R \hat{R}|0\rangle \tag{15}$$

where ΔE_R is the excited-state CC correlation energy. The excitation energy can be written as

$$\omega = E_R - E = \Delta E_R - \Delta E \tag{16}$$

After performing some algebra, we obtain the EOM-CCSD equation as follows:

$$(\hat{\mathcal{H}}\hat{R}|0\rangle)_C = \omega \hat{R}|0\rangle \tag{17}$$

Equation 17 is equivalent to the following matrix eigenvalue equation for CCSD:

$$\begin{pmatrix} 0 & \mathcal{H}_{0S} & \mathcal{H}_{0D} \\ 0 & \mathcal{H}_{SS} & \mathcal{H}_{SD} \\ 0 & \mathcal{H}_{DS} & \mathcal{H}_{DD} \end{pmatrix} \begin{pmatrix} R_0 \\ R_1 \\ R_2 \end{pmatrix} = \omega \begin{pmatrix} R_0 \\ R_1 \\ R_2 \end{pmatrix} \tag{18}$$

However, we solve eq 18 iteratively with the Davidson algorithm.[74−77] Hence, we need to introduce the so-called **σ** vector as follows:

$$\sigma_I = \sum_J \mathcal{H}_{IJ} R_J \tag{19}$$

where $I, J = 0, S, D$.

3.1. DF-EOM-CCSD Intermediates. The DF-CCSD intermediates that appear in the DF-EOM-CCSD equations are given in Appendix A.

3.1.1. DF-EOM-CCSD 3-Index Intermediates. 1- and 3-index intermediates that were used for EOM-CCSD are defined as follows:

$$r^Q = \sum_m^{occ} \sum_e^{vir} r_m^e b_{me}^Q \tag{20}$$

$$r_{ia}^Q = \sum_e^{vir} r_i^e b_{ae}^Q \tag{21}$$

$$r_{ij}^Q = \sum_e^{vir} r_i^e b_{je}^Q \tag{22}$$

$$r_{ai}^Q = \sum_m^{occ} r_m^a b_{im}^Q \tag{23}$$

$$r_{ab}^Q = \sum_m^{occ} r_m^a b_{mb}^Q \tag{24}$$

$$\tilde{r}_{ia}^Q = \sum_e^{vir} r_i^e t_{ae}^Q \tag{25}$$

$$\tilde{r}_{ai}^Q = \sum_m^{occ} r_m^a t_{im}^Q \tag{26}$$

$$r_{ia}^{Q'} = \sum_m^{occ} r_{im}^Q t_m^a \tag{27}$$

$$R_{ia}^Q = \sum_m^{occ} \sum_e^{vir} r_{im}^{ae} b_{me}^Q \tag{28}$$

where Q runs over auxiliary basis functions and the b_{pq}^Q terms are the molecular orbital (MO) basis DF factors, which are defined in our previous studies.[65−67]

3.1.2. 4-Index Intermediates. 4-index intermediates are defined as follows:

$$\mathcal{V}_{ijmn} = \sum_{e,f}^{vir} r_{ij}^{ef} \langle mn|ef \rangle_{DF} \tag{29}$$

$$\mathcal{V}_{ijam} = \sum_{e,f}^{vir} r_{ij}^{ef} \langle am|ef \rangle_{DF} \tag{30}$$

$$R_{mnij} = P_-(mn) \sum_Q^{aux} r_{im}^Q \{b_{jn}^Q + t_{jn}^Q\} \tag{31}$$

$$R_{mbif} = P_-(mb) \sum_Q^{aux} r_{im}^Q b_{bf}^Q \tag{32}$$

$$R_{mbij} = \sum_e^{vir} r_i^e \mathcal{Z}_{mbej} \tag{33}$$

3.1.3. 2-Index Intermediates. 2-index intermediates are defined as follows:

$$R_{im} = \sum_e^{vir} r_i^e \mathcal{F}_{me} \tag{34}$$

$$X_{ij} = \sum_Q^{aux} \sum_e^{vir} (R_{ie}^Q - r_{ei}^Q - \tilde{r}_{ei}^Q) b_{je}^Q + \sum_Q^{aux} (t_{ij}^Q + b_{ij}^Q) r^Q \tag{35}$$

$$X_{ab} = \sum_Q^{aux} \sum_m^{occ} (R_{ma}^Q + r_{ma}^Q - \tilde{r}_{ma}^Q) b_{mb}^Q + \sum_Q^{aux} (t_{ab}^Q - b_{ab}^Q) r^Q \tag{36}$$

3.2. DF-EOM-CCSD σ Equations. The DF-EOM-CCSD σ_0 equation can be written as

$$\sigma_0 = \sum_i^{occ} \sum_a^{vir} r_i^a F_{ia} + \frac{1}{4} \sum_{ij}^{occ} \sum_{ab}^{vir} r_{ij}^{ab} \langle ij||ab \rangle \tag{37}$$

With the DF approximation, the EOM-CCSD σ_i^a equation can be written as

$$\sigma_i^a = \sum_e^{vir} r_i^e \mathcal{F}_{ae} - \sum_m^{occ} r_m^a \mathcal{F}_{mi} + \sum_m^{occ} \sum_e^{vir} r_m^e \mathcal{W}_{maei}$$
$$+ \sum_m^{occ} \sum_e^{vir} r_{im}^{ae} F_{me} - \sum_Q^{aux} \sum_m^{occ} (t_{im}^Q + b_{im}^Q) R_{ma}^Q$$
$$+ \sum_Q^{aux} \sum_e^{vir} R_{ie}^Q (b_{ae}^Q - t_{ae}^Q) \tag{38}$$

With the DF approximation, the EOM-CCSD σ_{ij}^{ab} equation can be written as

$$\sigma_{ij}^{ab} = P_-(ab) \sum_e^{vir} r_{ij}^{eb} \mathcal{F}_{ae} - P_-(ij) \sum_m^{occ} r_{mj}^{ab} \mathcal{F}_{mi}$$
$$+ \frac{1}{2} \sum_{e,f}^{vir} r_{ij}^{ef} W_{abef} - P_-(ab) \sum_m^{occ} r_m^a \mathcal{W}_{mbij}$$
$$+ \frac{1}{2} \sum_{m,n}^{occ} \tau_{mn}^{ab} (R_{mnij} - R_{mnji} + \mathcal{V}_{ijmn}) + \frac{1}{2} \sum_{m,n}^{occ} r_{mn}^{ab} W_{mnij}$$
$$+ P_-(ij) P_-(ab) \sum_m^{occ} \sum_e^{vir} r_{im}^{ae} \mathcal{W}_{mbej}$$
$$- P_-(ij) P_-(ab) \sum_m^{occ} \sum_e^{vir} t_{im}^{ae} R_{mbje}$$
$$+ P_-(ij) P_-(ab) \sum_Q^{aux} r_{ia}^Q (b_{jb}^Q + t_{jb}^Q - \tilde{t}_{jb}^Q)$$
$$+ P_-(ij) P_-(ab) \sum_Q^{aux} r_{ib}^{Q'} t_{ja}^Q - P_-(ij) \sum_m^{occ} t_{mj}^{ab} R_{im}$$
$$- P_-(ij) P_-(ab) \sum_m^{occ} t_m^a R_{mbij} + P_-(ab) \sum_e^{vir} X_{ae} t_{ij}^{be}$$
$$+ P_-(ij) \sum_m^{occ} X_{im} t_{jm}^{ab} \tag{39}$$

3.3. PPL Algorithm with the DF Approach. The most expensive terms of the T_2 and σ_2 amplitude equations are the PPL terms. Our PPL algorithm for the σ_2 tensor originated from the PPL algorithm used for the T_2 amplitude equation in our 2016 study.[65] Here, we employ the same algorithm to σ_2 amplitudes. For example, for the closed-shell case, the PPL term can be written as

$$\sigma_{ij}^{ab} \leq \sum_{e,f}^{vir} r_{ij}^{ef} W_{abef} \tag{40}$$

Following the previous studies of Saebø and Pulay[78] and Scuseria at al.[79] and our previous DF-CCSD studies,[65,66] we employ the following algorithm for the evaluation of σ-PPL:

$$\sigma_{ij}^{ab} D_{ij}^{ab} \leq \sum_{e,f}^{vir} r_{ij}^{ef} W_{ef}^{ab} = S_{ij}^{ab} + A_{ij}^{ab} \tag{41}$$

where S is the symmetric component, while A is the antisymmetric component. Now let us define

$$^{(\pm)}r_{ij}^{ef} = \frac{1}{2}(r_{ij}^{ef} \pm r_{ji}^{ef}) \tag{42}$$

$$^{(\pm)}\tilde{r}_{ij}^{ef} = {}^{(\pm)}r_{ij}^{ef}(2 - \delta_{ef}) \tag{43}$$

$$^{(\pm)}W_{ef}^{ab} = \frac{1}{2}(W_{ef}^{ab} \pm W_{fe}^{ab}) \tag{44}$$

$$S_{ij}^{ab} = \sum_{e \geq f}^{vir} {}^{(+)}\tilde{r}_{ij}^{ef(+)} W_{ef}^{ab} \tag{45}$$

$$A_{ij}^{ab} = \sum_{e \geq f}^{vir} {}^{(-)}\tilde{r}_{ij}^{ef(-)} W_{ef}^{ab} \tag{46}$$

where S and A have the following symmetry properties.

$$S_{ij}^{ab} = S_{ji}^{ab} = S_{ij}^{ba} = S_{ji}^{ba} \tag{47}$$

$$A_{ij}^{ab} = -A_{ji}^{ab} = -A_{ij}^{ba} = A_{ji}^{ba} \tag{48}$$

Hence, we can always keep $i \geq j$ and $a \geq b$.

$$S_{i \geq j}^{a \geq b} = \sum_{e \geq f}^{vir} {}^{(+)}\tilde{r}_{i \geq j}^{e \geq f(+)} W_{e \geq f}^{a \geq b} \tag{49}$$

$$A_{i \geq j}^{a \geq b} = \sum_{e \geq f}^{vir} {}^{(-)}\tilde{r}_{i \geq j}^{e \geq f(-)} W_{e \geq f}^{a \geq b} \tag{50}$$

The pseudo code for the σ-PPL algorithm is

loop over a from 0 to $vir - 1$

    // Form $J^a(bfe) = (ae|bf)$, cost: $V^4 N_{aux}/2$

$$J^a(bfe) = \sum_Q B(bfQ) \times [B(aeQ) - T(aeQ)]$$

    // Form $J^a(mfe) = (mf|ae)$, cost: $OV^3 N_{aux}$

$$J^a(mfe) = \sum_Q B(mfQ) \times B(aeQ)$$

    // Form $J^a(bfe)$, cost: OV^4

$$J^a(bfe) = J^a(bfe) - \sum_m t(m, b) \times J^a(mfe)$$

    // Form $^{(\pm)}W^a(b, e \geq f)$, cost: $V^4/4$

$$^{(\pm)}W^a(b, e \geq f) = \frac{1}{2}[J^a(bef) \pm J^a(bfe)]$$

    // Form $S^a(b, i \geq j)$, $A^a(b, i \geq j)$, cost: $O^2 V^4/4$

$$S^a(b, i \geq j) = \sum_{e \geq f} {}^{(+)}\tilde{r}_{i \geq j}^{e \geq f} \times {}^{(+)}W^a(b, e \geq f)$$

$$A^a(b, i \geq j) = \sum_{e \geq f} {}^{(-)}\tilde{r}_{i \geq j}^{e \geq f} \times {}^{(-)}W^a(b, e \geq f)$$

end loop $\tag{51}$

With this algorithm, the cost of PPL is $1/4 O^2 V^4 + 1/2 V^4 N_{aux} + OV^3 N_{aux} + OV^4 + 1/4 V^4$. The most expensive term is $1/2 V^4 N_{aux}$. Finally, we note that our DF-EOM-CCSD code has a shared-memory parallelism feature through threaded BLAS calls as well as OPENMP parallelization of all tensor manipulations.

3.3.1. DF/CD Hybrid PPL Algorithm. In the common CD approach for ERIs, the CD factors are generated from the AO basis ERI tensor $(\mu\nu|\lambda\sigma)$, and the number of CD factors is generally higher than that of DF factors. Hence, it does not seem to speed up our DF algorithm. However, we have observed that, for the large molecules, the CD technique can be beneficial to take advantage of the sparsity of the ERI tensor if it is applied to the MO basis ERIs generated from the DF integrals. More specifically, if we perform the Cholesky decomposition of the $(ab|cd)$-type integrals, we may get a reduced number of auxiliary basis functions, which is especially true for large molecular systems. Hence, in our DF/CD hybrid approach, we build the $(ab|cd)$-type integrals from the DF factors, on-the-fly, and perform Cholesky decomposition simultaneously.

4. RESULTS AND DISCUSSION

Results from the DF-EOM-CCSD and RI-EOM-CCSD[80] methods were obtained for a set of alkanes to compare the computational cost for the excitation energy computations. For the alkanes set, Dunning's correlation-consistent polarized valence triple-ζ basis set (aug-cc-pVTZ) was used with the frozen core approximation.[81,82] For the aug-cc-pVTZ basis sets, aug-cc-pVTZ-JKFIT[50] and aug-cc-pVTZ-RI[83] auxiliary basis set pairs were employed for reference and correlation energies, respectively. Additionally, the DF-EOM-CCSD, resolution of the identity EOM-CCSD (RI-EOM-CCSD),[80] and EOM-CCSD(fT)[84] methods were applied to a set of molecules to compare the excitation energies.

4.1. Efficiency of DF-EOM-CCSD. A set of alkanes is considered to assess the efficiency of the RI-EOM-CCSD and DF-EOM-CCSD methods. The RI-EOM-CCSD computations were performed with the Q-CHEM 5.3 package.[72] The computational time for the RI-EOM-CCSD and DF-EOM-CCSD methods are presented graphically in Figures 1 and 2 for
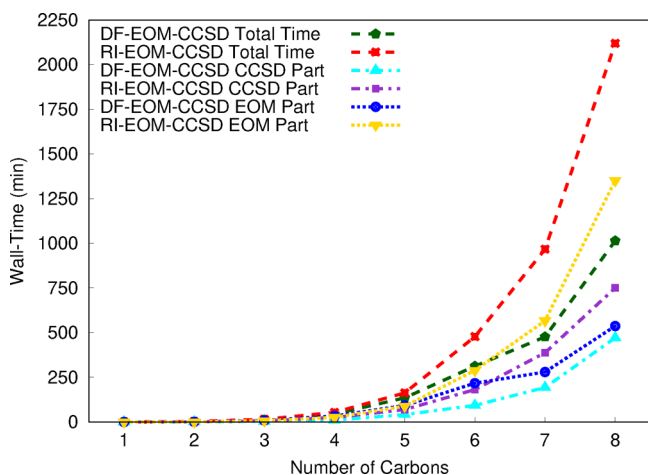

Figure 1. Total, CCSD, and EOM wall times (in min) for computations of excitation energies for the C_nH_{2n+2} ($n = 1-8$) set from the RI-EOM-CCSD (from Q-CHEM[72]) and DF-EOM-CCSD methods with the cc-pVTZ basis set. The RHF reference is used for these computations. All computations were performed for a single root with 10^{-7} energy and EOM eigenvalue convergence tolerances on a single node (1 core) Intel(R) Xeon(R) CPU E5-2620 v4 @ 2.10 GHz computer (memory ∼ 64 GB).
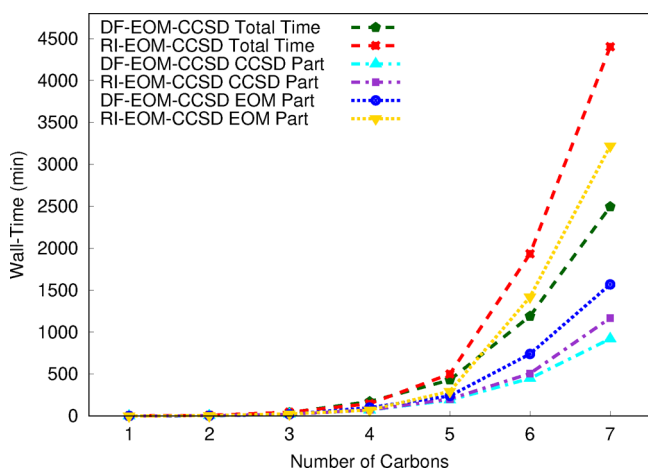

Figure 2. Total, CCSD, and EOM wall time (in min) for computations of excitation energies for the C_nH_{2n+2} ($n = 1-7$) set from the RI-EOM-CCSD (from Q-CHEM[72]) and DF-EOM-CCSD methods with the cc-pVTZ basis set. The UHF reference is used for these computations. All computations were performed for a single root with 10^{-7} energy and EOM eigenvalue convergence tolerances on a single node (1 core) Intel(R) Xeon(R) CPU E5-2620 v4 @ 2.10 GHz computer (memory ∼ 64 GB).

restricted and unrestricted Hartree-Fock (RHF and UHF) references, respectively. Timing computations were carried out for a single root with a 10^{-7} energy and 10^{-7} EOM eigenvalue convergence tolerances on a single node (1 core) Intel(R) Xeon(R) CPU E5-2620 v4 @ 2.10 GHz computer (memory ∼ 64 GB). For the RI-CCSD code of Q-CHEM 5.3, MEM_TOTAL

64000, MEM_STATIC 2000, and CC_MEMORY 51200 options are used. We start our assessment with the RHF versions of the RI-EOM-CCSD and DF-EOM-CCSD implementations. The DF-EOM-CCSD method significantly reduces the computational cost compared to RI-EOM-CCSD, and there is more than a 2-fold reduction in the computational time for DF-EOM-CCSD for the largest member (C_8H_{18}) of the alkanes set. For the C_8H_{18} molecule, the CCSD times are 750 and 471 min for RI-EOM-CCSD and DF-EOM-CCSD, respectively; there is a 1.6-fold reduction in the computational time for DF-EOM-CCSD. Further, for the C_8H_{18} molecule, the EOM times are 1351 min (RI-EOM-CCSD) and 537 min (DF-EOM-CCSD); hence, there is a 2.5-fold reduction in the computational time for DF-EOM-CCSD.

The number of iterations for the CCSD part are 11 (DF-EOM-CCSD) and 12 (RI-EOM-CCSD). The average computational time per CCSD iteration (t_{ccsd}/n_{iter}) for C_8H_{18} is 42.8 min (DF-EOM-CCSD) and 62.5 min (RI-EOM-CCSD). Hence, our new DF-EOM-CCSD implementation is 1.5 times faster than the RI-EOM-CCSD code for average computational cost per CCSD iteration. Similarly, the number of Davidson iterations for the EOM part is 12 (DF-EOM-CCSD) and 18 (RI-EOM-CCSD). The average computational time per a Davidson iteration (t_{eom}/n_{iter}) for C_8H_{18} is 44.8 min (DF-EOM-CCSD) and 75.1 min (RI-EOM-CCSD). Hence, our new DF-EOM-CCSD implementation is 1.7 times faster than the RI-EOM-CCSD code for average computational cost per EOM-CCSD iteration.

The efficiency of our DF-EOM-CCSD method compared to that of RI-EOM-CCSD is attributed to the our more efficient PPL algorithm. For the closed-shell case, the number of flops (NOF) for our DF-CCSD method[65,66] is $1/4O^2V^4 + 2O^3V^3 + 1/4O^4V^2$, while that of RI-CCSD[80] was reported to be $5/8O^2V^4 + 4O^3V^3 + 27/8O^4V^2$. When one compares the cost of implementation, our DF-CCSD implementation[65,66] is 2.5 times more efficient than that of RI-CCSD[80] for the PPL contraction term. Further, our implementation is 2 times more efficient compared to that of RI-CCSD for the particle-hole ladder (PHL) terms. Moreover, the cost of $VVVV$-type integral transformation, on-the-fly of course, is $1/2V^4N_{aux}$ in our case, while it appears to be V^4N_{aux} for RI-CCSD.[80] In fact, the most expensive term is this integral transformation step for large-scale computations with optimized auxiliary basis sets. Hence, our algorithm appears to be 2 times more efficient for this term. Basically, we follow the same algorithm for the PPL term of EOM; the same is also true for RI-EOM-CCSD. Hence, the efficiency of our DF-EOM-CCSD implementation was maintained.

As the second step of our timing assessment, we consider the UHF versions of the RI-EOM-CCSD and DF-EOM-CCSD implementations. The DF-EOM-CCSD method noticeably reduces the computational cost compared with RI-EOM-CCSD (Figure 2); there is a 1.8-fold reduction in the computational time for DF-EOM-CCSD for the C_7H_{16} molecule. For the C_7H_{16} molecule, the CCSD time is 1168 and 920 min for RI-EOM-CCSD and DF-EOM-CCSD, respectively; there is a 1.3-fold reduction in the computational time for DF-EOM-CCSD. Further, for the C_7H_{16} molecule, the EOM time is 3221 min (RI-EOM-CCSD) and 1568 min (DF-EOM-CCSD); hence, there is a 2.1-fold reduction in the computational time for DF-EOM-CCSD. The number of iterations for the UHF-CCSD part are 11 (DF-EOM-CCSD) and 12 (RI-EOM-CCSD) for the C_7H_{16} molecule. The average

computational time per UHF-CCSD iteration (t_{ccsd}/n_{iter}) for C_7H_{16} is 83.7 min (DF-EOM-CCSD) and 97.3 min (RI-EOM-CCSD). Hence, our new DF-EOM-CCSD implementation is 1.2 times faster than the RI-EOM-CCSD code for the average computational cost per UHF-CCSD iteration. Similarly, the number of Davidson iterations for the EOM part are 12 (DF-EOM-CCSD) and 18 (RI-EOM-CCSD). The average computational time per Davidson iteration (t_{eom}/n_{iter}) for C_7H_{16} is 130.7 min (DF-EOM-CCSD) and 178.9 min (RI-EOM-CCSD). Hence, our new DF-EOM-CCSD implementation is 1.4 times faster than the RI-EOM-CCSD code for the average computational cost per EOM-CCSD iteration. Hence, our new DF-EOM-CCSD implementation maintains its efficiency for the UHF reference.

4.1.1. Assessment of the DF/CD Hybrid PPL Algorithm. As the final step of our assessment for the efficiency of our new implementations, we present benchmark timing results for comparisons of DF and DF/CD hybrid approaches for the evaluation of the PPL terms of the CCSD and EOM parts. The ratios of the number of auxiliary basis functions employed in the PPL term of EOM-CCSD for the DF and DF/CD approaches are presented graphically in Figure 3. Since the most expensive
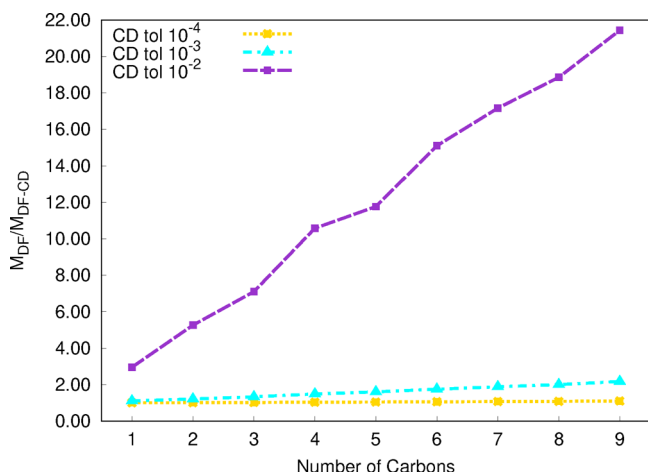

Figure 3. Ratio of the number of auxiliary basis functions, *M*, employed in the PPL term of DF-EOM-CCSD from the DF and hybrid DF/CD approaches (with the CD tolerances of 10^{-4}, 10^{-3}, and 10^{-2}) for computations of excitation energies for the C_nH_{2n+2} ($n = 1-9$) set. The RHF reference is used for these computations along with the cc-pVTZ basis set.

term of the PPL algorithm scales linearly with the number of auxiliary basis functions, lets call it *M*, the reduction of *M* may yield significant improvements in the evaluation of the PPL term. For example, for the C_9H_{20} molecule with the cc-pVTZ primary basis set, the *M* values are 1329 and 1208 for our canonical DF and hybrid DF/CD algorithms, respectively. Hence, the ratio of $M_{DF}/M_{DF/CD}$ is 1.10, which indicates a more than 10% reduction in the number of auxiliary basis functions. For the alkanes set considered, C_nH_{2n+2} ($n = 1-9$), we plot the $M_{DF}/M_{DF/CD}$ values with respect to the *n* values and obtain a linear relation for this fit. The equation and the R^2 value for the linear fit are $M_{DF}/M_{DF/CD} = 0.0122n + 0.9883$ and $R^2 = 0.9939$. At first, one should note that as the *n* value increases the $M_{DF}/M_{DF/CD}$ ratio increases as well. The reason for this correlation is that as molecular size increases the hybrid DF/CD algorithm makes better use of the sparsity of the ERI tensor. Hence, the obtained linear equation indicates that, if we proceed to larger

molecules, the hybrid DF/CD algorithm will have a larger impact on the computational time. For example, the $M_{DF}/M_{DF/CD}$ ratio will be approximately 1.23 and 1.60 for the $C_{20}H_{42}$ and $C_{50}H_{102}$ molecules, which indicates up to 23% and 60% acceleration in the PPL terms can be achieved.

For the alkanes set, the computational time for the DF-EOM-CCSD and hybrid DF/CD-EOM-CCSD approaches with the CD tolerances of 10^{-4}, 10^{-3}, and 10^{-2} are presented graphically in Figure 4. For the largest member of the test set, C_9H_{20}, the
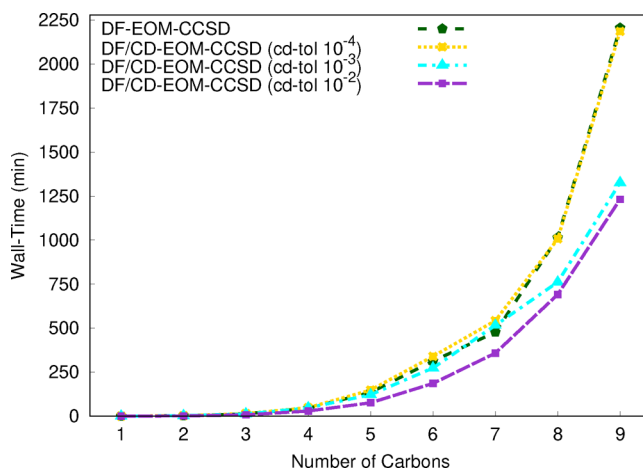

Figure 4. Total wall time (in min) for computations of excitation energies for the C_nH_{2n+2} ($n = 1-9$) set from the DF-EOM-CCSD and hybrid DF/CD-EOM-CCSD (with the CD tolerances of 10^{-4}, 10^{-3}, and 10^{-2}) methods with the cc-pVTZ basis set. The RHF reference is used for these computations. All computations were performed for a single root with 10^{-7} energy and EOM eigenvalue convergence tolerances on a single node (1 core) Intel(R) Xeon(R) CPU E5-2620 v4 @ 2.10 GHz computer (memory ∼ 64 GB).

computational times are 2205.9 min (DF-EOM-CCSD), 2186.6 min (DF/CD-EOM-CCSD with $tol_{CD} = 10^{-4}$), 1326.6 min (DF/CD-EOM-CCSD with $tol_{CD} = 10^{-3}$), and 1232.0 min (DF/CD-EOM-CCSD with $tol_{CD} = 10^{-2}$). With $tol_{CD} = 10^{-4}$, the cost of DF/CD-EOM-CCSD is slightly reduced compared with that of DF-EOM-CCSD, while with $tol_{CD} = 10^{-3}$ and $tol_{CD} = 10^{-2}$, the cost of DF/CD-EOM-CCSD is reduced 39.9% and 44.1% compared with that of the canonical DF-EOM-CCSD. Hence, our new hybrid approach provides significant improvements in efficiency compared to the that of the canonical DF algorithm. Further, our above discussion suggests that for the larger molecules further improvements may be observed. Hence, our new hybrid DF/CD PPL algorithm appears to be very promising for large-sized chemical systems.

We would like to note why we did not prefer the CD decomposition of the original 4-index ERIs. The number of CD factors generated from the 4-index ERIs are generally much higher than that of the DF factors achieving the same accuracy. For example, for the C_8H_{18} molecule with the cc-pVTZ basis set, the number of auxiliary basis functions are 1188 (DF), 2018 ($tol_{CD} = 10^{-4}$), 1621 ($tol_{CD} = 10^{-3}$), and 1005 ($tol_{CD} = 10^{-2}$). Hence, the number auxiliary basis functions obtained from the partial CD decomposition of the conventional 4-index ERIs may yield a similar number with DF only if it is used with a loose CD tolerance of 10^{-2}. However, with our hybrid approach, the number of auxiliary basis functions are 1095 ($tol_{CD} = 10^{-4}$), 593 ($tol_{CD} = 10^{-3}$), and 63 ($tol_{CD} = 10^{-2}$). Hence, our hybrid DF/CD

Table 1. Excitation Energies for the First Five Excited States (in eV) of the Test Set Considered from the DF-EOM-CCSD, DF/CD-EOM-CCSD, RI-EOM-CCSD, and EOM-CCSD(fT) Methods with the aug-cc-pVTZ Basis Set

	DF-EOM-CCSD	DF/CD-EOM-CCSD[a]	DF/CD-EOM-CCSD[b]	DF/CD-EOM-CCSD[c]	DF/CD-EOM-CCSD[d]	DF/CD-EOM-CCSD[e]	RI-EOM-CCSD[f]	EOM-CCSD(fT)[f]
1	5.78	5.78	5.78	5.78	5.78	5.79	5.83	5.51
	6.67	6.67	6.67	6.68	6.71	6.73	6.70	6.41
	6.72	6.72	6.72	6.73	6.75	6.78	6.72	6.47
	7.33	7.33	7.33	7.33	7.34	7.36	7.39	7.07
	7.69	7.69	7.70	7.70	7.73	7.76	7.73	7.48
2	4.53	4.53	4.53	4.53	4.53	4.54	4.57	4.25
	6.57	6.57	6.57	6.58	6.61	6.63	6.60	6.36
	7.55	7.55	7.55	7.56	7.59	7.62	7.58	7.36
	7.60	7.60	7.61	7.61	7.64	7.67	7.63	7.40
	7.68	7.68	7.68	7.69	7.72	7.75	7.71	7.50
3	5.69	5.69	5.70	5.70	5.75	5.78	5.70	5.30
	5.87	5.87	5.88	5.89	5.96	6.01	5.86	5.58
	6.49	6.49	6.50	6.50	6.58	6.64	6.47	6.21
	6.54	6.54	6.55	6.56	6.63	6.69	6.52	6.25
	6.65	6.65	6.65	6.66	6.74	6.79	6.63	6.36
4	6.79	6.79	6.79	6.79	6.81	6.84	6.80	6.50
	6.92	6.92	6.92	6.92	6.95	6.98	6.91	6.62
	7.03	7.03	7.04	7.04	7.09	7.13	7.02	6.80
	7.42	7.42	7.42	7.43	7.47	7.51	7.41	7.18
	7.45	7.45	7.45	7.46	7.50	7.54	7.43	7.21
5	6.36	6.36	6.36	6.37	6.42	6.47	6.39	6.02
	6.45	6.45	6.45	6.46	6.53	6.60	6.43	6.16
	6.76	6.76	6.76	6.77	6.84	6.91	6.74	6.47
	6.92	6.92	6.93	6.93	7.00	7.08	6.90	6.63
	7.21	7.21	7.22	7.22	7.28	7.34	7.18	6.69
6	7.48	7.48	7.49	7.49	7.51	7.54	7.46	7.23
	8.09	8.09	8.09	8.09	8.10	8.12	8.08	7.81
	8.13	8.13	8.13	8.13	8.16	8.19	8.11	7.89
	8.20	8.20	8.20	8.20	8.23	8.26	8.18	7.95
	8.55	8.55	8.55	8.56	8.57	8.59	8.56	8.36
7	4.07	4.07	4.07	4.07	4.07	4.07	4.07	3.82
	7.20	7.20	7.20	7.20	7.21	7.22	7.22	7.07
	8.09	8.09	8.09	8.09	8.09	8.10	8.11	7.97
	8.18	8.18	8.18	8.18	8.19	8.21	8.20	8.07
	8.61	8.61	8.61	8.61	8.62	8.63	8.64	8.52
8	5.70	5.70	5.70	5.70	5.70	5.70	5.74	5.45
	6.92	6.92	6.93	6.93	6.94	6.96	6.92	6.68
	6.99	6.99	7.00	7.00	7.01	7.03	7.01	6.71
	7.51	7.51	7.51	7.51	7.52	7.54	7.57	7.31
	7.71	7.71	7.71	7.72	7.73	7.74	7.76	7.53
9	6.19	6.19	6.20	6.20	6.27	6.32	6.18	5.88
	6.57	6.57	6.57	6.58	6.62	6.65	6.53	6.09
	6.73	6.73	6.74	6.74	6.81	6.86	6.72	6.43
	6.89	6.89	6.89	6.89	6.91	6.93	6.90	6.60
	6.92	6.92	6.92	6.93	7.00	7.05	7.34	7.03
10	5.82	5.82	5.83	5.84	5.89	5.93	5.81	5.50
	6.59	6.59	6.60	6.60	6.65	6.70	6.58	6.29
	6.63	6.63	6.63	6.63	6.67	6.70	6.59	6.16
	6.85	6.85	6.85	6.86	6.89	6.90	6.83	6.54
	6.87	6.87	6.87	6.88	6.91	6.96	6.91	6.49

[a]These computations were performed with the hybrid DF/CD algorithm employing a CD tolerance of 1×10^{-4}. [b]These computations were performed with the hybrid DF/CD algorithm employing a CD tolerance of 5×10^{-4}. [c]These computations were performed with the hybrid DF/CD algorithm employing a CD tolerance of 1×10^{-3}. [d]These computations were performed with the hybrid DF/CD algorithm employing a CD tolerance of 5×10^{-3}. [e]These computations were performed with the hybrid DF/CD algorithm employing a CD tolerance of 1×10^{-2}. [f]These computations were performed with the Q-CHEM 5.3 program.

approach significantly reduces the number of auxiliary basis functions.

4.2. Accuracy of DF-EOM-CCSD.

In this section, we consider a test set to assess the accuracy of the DF-EOM-CCSD method. Chemical names of the molecules considered are given

in the Supporting Information. Excitation energies (in eV) for the test set considered from the DF-EOM-CCSD, DF/CD-EOM-CCSD, RI-EOM-CCSD, and EOM-CCSD(fT) methods with the aug-cc-pVTZ basis set are reported in Table 1. The mean absolute errors (MAEs) with respect to EOM-CCSD(fT) are depicted in Figure 5. The MAE values with respect to EOM-
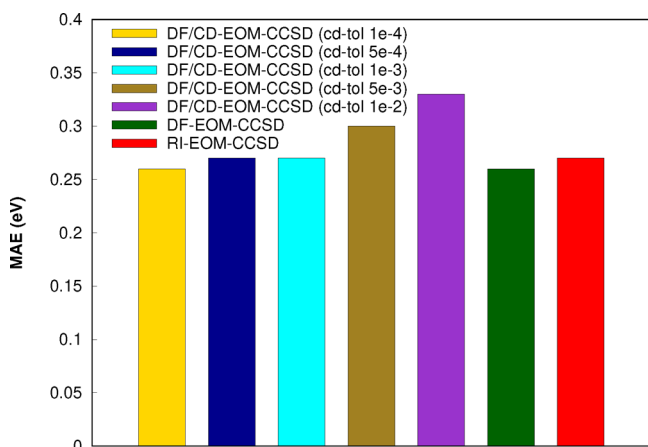

Figure 5. Mean absolute errors (in eV) in excitation energies for the test set from the DF-EOM-CCSD, DF/CD-EOM-CCSD, and RI-EOM-CCSD methods with respect to EOM-CCSD(fT) (the aug-cc-pVTZ basis set was employed).

CCSD(fT) are 0.71 eV (CIS), 0.26 eV (DF-EOM-CCSD), 0.26 eV (DF/CD-EOM-CCSD with $tol_{CD} = 10^{-4}$), 0.27 eV (DF/CD-EOM-CCSD with $tol_{CD} = 5 \times 10^{-4}$), 0.27 eV (DF/CD-EOM-CCSD with $tol_{CD} = 10^{-3}$), 0.30 eV (DF/CD-EOM-CCSD with $tol_{CD} = 5 \times 10^{-3}$), 0.33 eV (DF/CD-EOM-CCSD with $tol_{CD} = 10^{-2}$), and 0.27 (RI-EOM-CCSD). Hence, the results of DF-EOM-CCSD, RI-EOM-CCSD, and DF/CD-EOM-CCSD (with $tol_{CD} = 10^{-4}-10^{-3}$) are almost identical. Further, the errors of DF/CD-EOM-CCSD with $tol_{CD} = 5 \times 10^{-3}$ and 10^{-2} are only 0.03 and 0.06 eV, deviating from the DF-EOM-CCSD approach. When these results and the computational efficiency are considered, the DF/CD-EOM-CCSD approach may be used with such loose CD tolerances. The differences between DF-EOM-CCSD and RI-EOM-CCSD results are in between 0.00 and 0.06 eV for most cases.

5. CONCLUSIONS

In this study, a new implementation of the density-fitted EOM-CCSD (DF-EOM-CCSD) method has been presented with an enhanced algorithm for the particle–particle ladder (PPL) term, which is the most expensive term of the EOM-CCSD computations. To further improve the evaluation of the PPL term, a hybrid DF/CD algorithm has also been introduced. The computational time of the DF-EOM-CCSD excitation energies has been compared with that of the RI-EOM-CCSD method (from Q-CHEM 5.3 package[72]).

The DF-EOM-CCSD method significantly reduces the computational cost compared to that of the RI-EOM-CCSD method; there is more than a 2-fold reduction for the C_8H_{18} molecule in a cc-pVTZ basis set with the RHF reference. This cost savings results from the accelerated evaluation of the PPL term. In our RHF based DF-EOM-CCSD method, the number of flops (NOFs) for the PPL contraction term is 2.5 times lower than that of the RI-EOM-CCSD method. Further, the prefactor of the *VVVV*-type transformation step used in the PPL term has

a reduced NOF value by a factor of 2. For the UHF reference, our implementation maintains its better performance and provides a 1.8-fold reduction in the computational cost compared to that of the RI-EOM-CCSD method for the C_7H_{16} molecule. Furthermore, our results show that the suggested hybrid DF/CD algorithm further improves the canonical DF algorithm, and the degree of improvement increases as the molecular size increases. The preliminary results indicate that the new hybrid DF/CD PPL algorithm is very promising for large-sized chemical systems.

Finally, the DF-EOM-CCSD and DF/CD-EOM-CCSD methods are applied to a test set to compare the excitation energies with those from the CIS, RI-EOM-CCSD, and EOM-CCSD(fT) methods. Our results demonstrate that the DF-EOM-CCSD and DF/CD-EOM-CCSD methods (with CD tolerances of $10^{-4}-10^{-3}$) provide identical results with to those of the RI-EOM-CCSD method. Further, the DF/CD-EOM-CCSD approach yields tolerable errors (0.03 and 0.06 eV) compared with those of the DF-EOM-CCSD method for the test set considered with loose CD tolerances, such as 5×10^{-3} and 10^{-2}.

■ APPENDIX A

DF-CCSD 3-Index Intermediates. 1- and 3-index intermediates used for DF-CCSD are given as follows:[65,66]

$$T_{ia}^Q = \sum_j^{occ} \sum_b^{vir} t_{ij}^{ab} b_{jb}^Q \tag{52}$$

$$t_Q = \sum_m^{occ} \sum_f^{vir} t_m^f b_{mf}^Q \tag{53}$$

$$t_{ia}^Q = \sum_f^{vir} t_i^f b_{af}^Q \tag{54}$$

$$t_{ij}^Q = \sum_e^{vir} t_i^e b_{je}^Q \tag{55}$$

$$t_{ai}^Q = \sum_m^{occ} t_m^a b_{mi}^Q \tag{56}$$

$$t_{ab}^Q = \sum_m^{occ} t_m^a b_{mb}^Q \tag{57}$$

$$\tilde{\tau}_{ia}^Q = \sum_m^{occ} \sum_f^{vir} \tilde{\tau}_{im}^{af} b_{mf}^Q \tag{58}$$

$$\tilde{t}_{ia}^Q = \sum_m^{occ} t_{im}^Q t_m^a \tag{59}$$

$$t_{ia}^{Q'} = t_{ia}^Q - t_{ai}^Q - \tilde{t}_{ia}^Q \tag{60}$$

$$\tau_{ia}^{Q'} = \tilde{\tau}_{ia}^Q + t_{ia}^Q \tag{61}$$

$$\tau_{ia}^{Q''} = \tilde{\tau}_{ia}^Q - t_{ai}^Q \tag{62}$$

where

$$\tilde{\tau}_{ij}^{ab} = t_{ij}^{ab} + \frac{1}{2}(t_i^a t_j^b - t_i^b t_j^a) \tag{63}$$

and b_{rs}^Q values are the molecular orbital (MO) DF factors, which are defined in our previous studies.[65−67]

F and $\mathcal{F}$ Intermediates. Density-fitted F and $\mathcal{F}$ intermediates are[65,66]

$$F_{mi} = f_{mi} + \frac{1}{2}\sum_e^{vir} f_{me}t_i^e + \sum_Q^{N_{aux}} t_Q b_{mi}^Q + \sum_Q^{N_{aux}}\sum_e^{vir} \tau_{ie}^{Q''} b_{me}^Q \tag{64}$$

$$F_{ae} = f_{ae} - \frac{1}{2}\sum_m^{occ} f_{me}t_m^a + \sum_Q^{N_{aux}} t_Q b_{ae}^Q - \sum_Q^{N_{aux}}\sum_m^{occ} \tau_{ma}^{Q'} b_{me}^Q \tag{65}$$

$$F_{me} = f_{me} + \sum_Q^{N_{aux}} t_Q b_{me}^Q - \sum_Q^{N_{aux}}\sum_n^{occ} t_{nm}^Q b_{ne}^Q \tag{66}$$

$$\mathcal{F}_{mi} = F_{mi} + \frac{1}{2}\sum_e^{vir} t_i^e F_{me} \tag{67}$$

$$\mathcal{F}_{ae} = F_{ae} - \frac{1}{2}\sum_m^{occ} t_m^a F_{me} \tag{68}$$

where f_{pq} is the MO basis Fock matrix. We would like to note that in our previous studies[65,66] the diagonal parts of the Fock matrix were removed from the definitions of the F_{mi} and F_{ae} intermediates since the diagonal Fock terms were moved into the $t_{ij}^{ab} D_{ij}^{ab}$ definition in the amplitude equation.

W Intermediates. W intermediates, with the DF approximation, are[65,66]

$$W_{mnij} = \langle mn\|ij\rangle_{DF} + P_{-}(mn)P_{-}(ij)\sum_Q^{N_{aux}} t_{im}^Q b_{jn}^Q$$
$$+ \sum_e^{vir}\sum_f^{vir} \tau_{ij}^{ef}\langle mn|ef\rangle_{DF} \tag{69}$$

$$W_{abef} = \langle ab\|ef\rangle_{DF} - P_{-}(ab)\sum_m^{occ} t_m^b\langle am\|ef\rangle_{DF} \tag{70}$$

$$W_{mbej} = \langle mb\|ej\rangle_{DF} + \sum_Q^{N_{aux}}\left(t_{jb}^{Q'} + \frac{1}{2}T_{jb}^Q\right)b_{me}^Q$$
$$+ \sum_Q^{N_{aux}} t_{be}^Q(t_{jm}^Q + b_{jm}^Q) - \sum_Q^{N_{aux}} t_{jm}^Q b_{be}^Q$$
$$- \frac{1}{2}\sum_n^{occ}\sum_f^{vir} t_{jn}^{bf}\langle em|nf\rangle_{DF} \tag{71}$$

where $P_{\pm}(pq)$ is defined by

$$P_{\pm}(pq) = 1 \pm \mathcal{P}(pq) \tag{72}$$

and $\mathcal{P}(pq)$ acts to permute the indices p and q.

$\mathcal{Z}$ and $\mathcal{W}$ Intermediates. The $\mathcal{Z}$ and $\mathcal{W}$ intermediates are defined as follows:[65,66]

$$\mathcal{Z}_{mbej} = \langle mb\|ej\rangle_{DF} - \sum_n^{occ}\sum_f^{vir} t_{nj}^{bf}\langle mn\|ef\rangle_{DF} \tag{73}$$

$$\mathcal{W}_{mbej} = \mathcal{Z}_{mbej} + \sum_Q^{N_{aux}} t_{jb}^{Q'} b_{me}^Q + \sum_Q^{N_{aux}} t_{be}^Q(t_{jm}^Q + b_{jm}^Q)$$
$$- \sum_Q^{N_{aux}} t_{jm}^Q b_{be}^Q \tag{74}$$

$$\mathcal{W}_{mbij} = \langle mb\|ij\rangle_{DF} - \sum_e^{vir} t_{ij}^{be}\mathcal{F}_{me} - \sum_n^{occ} t_n^b\mathcal{W}_{mnij}$$
$$+ \sum_{e,f}^{vir} \tau_{ij}^{ef}\langle mb|ef\rangle_{DF} + P_{-}(ij)\sum_e^{vir} t_i^e \mathcal{Z}_{mbej}$$
$$+ P_{-}(ij)\sum_n^{occ}\sum_e^{vir} t_{jn}^{be}\langle mn\|ie\rangle_{DF} \tag{75}$$

ASSOCIATED CONTENT

ⓢ Supporting Information

The Supporting Information is available free of charge at https://pubs.acs.org/doi/10.1021/acs.jctc.1c01000.

Optimized geometries of the species; excitation energies with the cc-pVTZ basis set for the test set; CIS excitation energies with the aug-cc-pVTZ basis set for the test set (PDF)

Spin-free RHF-DF-EOM-CCSD equations (PDF)

AUTHOR INFORMATION

Corresponding Author

Uğur Bozkaya − *Department of Chemistry, Hacettepe University, Ankara 06800, Turkey;* ⓘ orcid.org/0000-0002-5203-2210; Email: ugur.bozkaya@hacettepe.edu.tr

Author

Aslı Ünal − *Graduate School of Science and Engineering, Hacettepe University, Ankara 06800, Turkey; Department of Chemistry, Hacettepe University, Ankara 06800, Turkey*

Complete contact information is available at:
https://pubs.acs.org/10.1021/acs.jctc.1c01000

Author Contributions

A.U.: Investigation, methodology, software, validation, and visualization. U.B: Conceptualization, funding acquisition, methodology, project administration, resources, software, supervision, and writing (original draft, review, and editing).

Notes

The authors declare no competing financial interest.

REFERENCES

(1) Cizek, J. On the Correlation Problem in Atomic and Molecular Systems. Calculation of Wavefunction Components in Ursell-Type Expansion Using Quantum-Field Theoretical Methods. *J. Chem. Phys.* **1966**, *45*, 4256.

(2) Bartlett, R. J. Many-Body Perturbation Theory and Coupled Cluster Theory for Electron Correlation in Molecules. *Annu. Rev. Phys. Chem.* **1981**, *32*, 359−401.

(3) Bartlett, R. J. Coupled-Cluster Approach to Molecular Structure and Spectra: A Step Toward Predictive Quantum Chemistry. *J. Phys. Chem.* **1989**, *93*, 1697−1708.

(4) Crawford, T. D.; Schaefer, H. F. An Introduction to Coupled Cluster Theory for Computational Chemists. *Rev. Comp. Chem.* **2007**, *14*, 33−136.

(5) Bartlett, R. J.; Musiał, M. Coupled-Cluster Theory in Quantum Chemistry. *Rev. Mod. Phys.* **2007**, *79*, 291−352.

(6) Bartlett, R. J. Coupled-Cluster Theory and Its Equation-of-Motion Extensions. *WIREs Comput. Mol. Sci.* **2012**, *2*, 126−138.

(7) Barlett, R. J.; Sekino, H.; Purvis, G. D. Comparison of MBPT and Coupled-cluster Methods with Full CI. Importance of Triplet Excitation and Infinite Summations. *Chem. Phys. Lett.* **1983**, *98*, 66−71.

(8) Lee, Y. S.; Kucharski, S. A.; Bartlett, R. J. A Coupled Cluster Approach with Triple Excitations. *J. Chem. Phys.* **1984**, *81*, 5906−5912.

(9) Pople, J. A.; Head-Gordon, M.; Raghavachari, K. Quadratic Configuration Interaction. A General Technique for Determining Electron Correlation Energies. *J. Chem. Phys.* **1987**, *87*, 5968−5975.

(10) Raghavachari, K.; Trucks, G. W.; Pople, J. A.; Head-Gordon, M. A Fifth-Order Perturbation Comparison of Electronic Correlation Theories. *Chem. Phys. Lett.* **1989**, *157*, 479−483.

(11) Bartlett, R. J.; Watts, J. D.; Kucharski, S. A.; Noga, J. Non-Iterative Fifth-Order Triple and Quadruple Excitation Energy Corrections in Correlated Methods. *Chem. Phys. Lett.* **1990**, *165*, 513−522.

(12) Scuseria, G. E.; Lee, T. J. Comparison of Coupled-Cluster Methods which Include the Effects of Connected Triple Excitations. *J. Chem. Phys.* **1990**, *93*, 5851−5855.

(13) Scuseria, G. E.; Hamilton, T. P.; Schaefer, H. F. An Assessment for the Full Coupled Cluster Method Including All Single, Double, and Triple Excitations: The Diatomic Molecules LiH, Li_2, BH, LiF, C_2, BeO, CN^+, BF, NO^+, and F_2. *J. Chem. Phys.* **1990**, *92*, 568−573.

(14) Purvis, G. D.; Bartlett, R. J. A Full Coupled-Cluster Singles and Doubles Model: The Inclusion of Disconnected Triples. *J. Chem. Phys.* **1982**, *76*, 1910−1918.

(15) Urban, M.; Noga, J.; Cole, S. J.; Bartlett, R. J. Towards a Full CCSDT Model for Electron Correlation. *J. Chem. Phys.* **1985**, *83*, 4041−4046.

(16) Lee, T. J.; Scuseria, G. E. In *Quantum Mechanical Electronic Structure Calculations with Chemical Accuracy*; Langhoff, S. R., Ed.; Kluwer Academic: Dordrecht, 1995; pp 47−108.

(17) Watts, J. D.; Stanton, J. F.; Bartlett, R. J. A Benchmark Coupled-Cluster Single, Double, and Triple Excitation (CCSDT) Study of the Structure and Harmonic Vibrational Frequencies of the Ozone Molecule. *Chem. Phys. Lett.* **1991**, *178*, 471−474.

(18) Scuseria, G. E. Ab Initio Theoretical Predictions of the Equilibrium Geometries of C_{60}, $C_{60}H_{60}$ and $C_{60}F_{60}$. *Chem. Phys. Lett.* **1991**, *176*, 423−427.

(19) Gauss, J.; Lauderdale, W. J.; Stanton, J. F.; Watts, J. D.; Bartlett, R. J. Analytic Energy Gradients for Open-Shell Coupled-Cluster Singles and Doubles (CCSD) Calculations Using Restricted Open-Shell Hartree−Fock (ROHF) Reference Functions. *Chem. Phys. Lett.* **1991**, *182*, 207−215.

(20) Watts, J. D.; Bartlett, R. J. Coupled-Cluster Calculations on the C_2 molecule and the C_2^+ and C_2^- Molecular Ions. *J. Chem. Phys.* **1992**, *96*, 6073−6084.

(21) Thomas, J. R.; DeLeeuw, B. J.; Vacek, G.; Crawford, T. D.; Yamaguchi, Y.; Schaefer, H. F. The Balance Between Theoretical Method and Basis Set Quality: A Systematic Study of Equilibrium Geometries, Dipole Moments, Harmonic Vibrational Frequencies, and Infrared Intensities. *J. Chem. Phys.* **1993**, *99*, 403−416.

(22) Watts, J. D.; Gauss, J.; Bartlett, R. J. Coupled-Cluster Methods With Noniterative Triple Excitations For Restricted Open-Shell Hartree-Fock And Other General Single Determinant Reference Functions. Energies And Analytical Gradients. *J. Chem. Phys.* **1993**, *98*, 8718−8733.

(23) Crawford, T. D.; Schaefer, H. F. A Comparison of Two Approaches to Perturbational Triples Corrections to the Coupled-Cluster Singles and Doubles Method for High-Spin Open-Shell Systems. *J. Chem. Phys.* **1996**, *104*, 6259−6264.

(24) Crawford, T. D.; Lee, T. J.; Schaefer, H. F. A New Spin-Restricted Perturbative Triple Excitation Correction for Coupled Cluster Theory. *J. Chem. Phys.* **1997**, *107*, 7943−7950.

(25) Bozkaya, U.; Schaefer, H. F. Symmetric and Asymmetric Triple Excitation Corrections for The Orbital-Optimized Coupled-Cluster Doubles Method: Improving Upon CCSD(T) and $CCSD(T)_\Lambda$: Preliminary Application. *J. Chem. Phys.* **2012**, *136*, 204114.

(26) Stanton, J. F.; Bartlett, R. J. The Equation of Motion Coupled-Cluster Method. A Systematic Biorthogonal Approach to Molecular Excitation Energies, Transition Probabilities, and Excited State Properties. *J. Chem. Phys.* **1993**, *98*, 7029−7039.

(27) Watts, J. D.; Bartlett, R. J. Economical Triple Excitation Equation-of-Motion Coupled-Cluster Methods for Excitation Energies. *Chem. Phys. Lett.* **1995**, *233*, 81−87.

(28) Gwaltney, S. R.; Nooijen, M.; Bartlett, R. J. Simplified Methods for Equation-of-Motion Coupled-Cluster Excited State Calculations. *Chem. Phys. Lett.* **1996**, *248*, 189−198.

(29) Hirata, S.; Nooijen, M.; Grabowski, I.; Bartlett, R. J. Perturbative Corrections to Coupled-Cluster and Equation-of-Motion Coupled-Cluster Energies: A Determinantal Analysis. *J. Chem. Phys.* **2001**, *114*, 3919−3928.

(30) Sattelmeyer, K. W.; Stanton, J. F.; Olsen, J.; Gauss, J. A Comparison of Excited State Properties for Iterative Approximate Triples Linear Response Coupled Cluster Methods. *Chem. Phys. Lett.* **2001**, *347*, 499−504.

(31) Larsen, H.; Hald, K.; Olsen, J.; Jørgensen, P. Triplet Excitation Energies in Full Configuration Interaction and Coupled-Cluster Theory. *J. Chem. Phys.* **2001**, *115*, 3015−3020.

(32) Hirata, S. Higher-Order Equation-of-Motion Coupled-Cluster Methods. *J. Chem. Phys.* **2004**, *121*, 51.

(33) Smith, C. E.; King, R. A.; Crawford, T. D. Coupled Cluster Methods Including Triple Excitations for Excited States of Radicals. *J. Chem. Phys.* **2005**, *122*, 054110.

(34) Gour, J. R.; Piecuch, P.; Włoch, M. Active-Space Equation-of-Motion Coupled-Cluster Methods for Excited States of Radicals and Other Open-Shell Systems: EA-EOMCCSDt and IP-EOMCCSDt. *J. Chem. Phys.* **2005**, *123*, 134113.

(35) Slipchenko, L. V.; Krylov, A. I. Spin-Conserving and Spin-Flipping Equation-of-Motion Coupled-Cluster Method with Triple Excitations. *J. Chem. Phys.* **2005**, *123*, 084107.

(36) Musiał, M.; Bartlett, R. J. Addition by Subtraction in Coupled Cluster Theory. II. Equation-of-Motion Coupled Cluster Method for Excited, Ionized, and Electron-Attached States Based on The nCC Ground State Wave Function. *J. Chem. Phys.* **2007**, *127*, 024106.

(37) Krylov, A. I. Equation-of-Motion Coupled-Cluster Methods for Open-Shell and Electronically Excited Species: The Hitchhiker's Guide to Fock Space. *Annu. Rev. Phys. Chem.* **2008**, *59*, 433−462.

(38) Musial, M.; Bartlett, R. J. Multireference Fock-Space Coupled-Cluster and Equation-of-Motion Coupled-Cluster Theories: The Detailed Interconnections. *J. Chem. Phys.* **2008**, *129*, 134105.

(39) Kuś, T.; Lotrich, V. F.; Bartlett, R. J. Parallel Implementation of The Equation-of-Motion Coupled-Cluster Singles and Doubles Method and Application for Radical Adducts of Cytosine. *J. Chem. Phys.* **2009**, *130*, 124122.

(40) Musiał, M. The Excited, Ionized and Electron Attached States Within The EOM-CC Approach with Full Inclusion of Connected Triple Excitations. *Mol. Phys.* **2010**, *108*, 2921−2931.

(41) Sneskov, K.; Christiansen, O. Excited State Coupled Cluster Methods. *Wiley Interdisciplinary Reviews: Computational Molecular Science* **2012**, *2*, 566−584.

(42) Bartlett, R. J. Coupled-Cluster Theory and Its Equation-of-Motion Extensions. *WIREs Computational Molecular Science* **2012**, *2*, 126−138.

(43) Musiał, M.; Olszówka, M.; Lyakh, D. I.; Bartlett, R. J. The Equation-of-Motion Coupled Cluster Method for Triple Electron Attached States. *J. Chem. Phys.* **2012**, *137*, 174102.

(44) Matthews, D. A.; Stanton, J. F. A New Approach to Approximate Equation-of-Motion Coupled Cluster with Triple Excitations. *J. Chem. Phys.* **2016**, *145*, 124102.

(45) Whitten, J. L. Coulombic Potential Energy Integrals and Approximations. *J. Chem. Phys.* **1973**, *58*, 4496−4501.

(46) Dunlap, B. I.; Connolly, J. W. D.; Sabin, J. R. On Some Approximations in Applications Xα Theory. *J. Chem. Phys.* **1979**, *71*, 3396−3402.

(47) Feyereisen, M.; Fitzgerald, G.; Komornicki, A. Use of Approximate Integrals in Ab Initio Theory. An Application in MP2 Energy Calculations. *Chem. Phys. Lett.* **1993**, *208*, 359−363.

(48) Vahtras, O.; Almlöf, J.; Feyereisen, M. W. Integral Approximations for LCAO-SCF Calculations. *Chem. Phys. Lett.* **1993**, *213*, 514−518.

(49) Rendell, A. P.; Lee, T. J. Coupled-Cluster Theory Employing Approximate Integrals: An Approach to Avoid The Input/Output and Storage Bottlenecks. *J. Chem. Phys.* **1994**, *101*, 400−408.

(50) Weigend, F. A Fully Direct RI-HF Algorithm: Implementation, Optimised Auxiliary Basis Sets, Demonstration of Accuracy and Efficiency. *Phys. Chem. Chem. Phys.* **2002**, *4*, 4285−4291.

(51) Sodt, A.; Subotnik, J. E.; Head-Gordon, M. Linear Scaling Density Fitting. *J. Chem. Phys.* **2006**, *125*, 194109.

(52) Werner, H.-J.; Manby, F. R.; Knowles, P. J. Fast Linear Scaling Second-Order Møller-Plesset Perturbation Theory (MP2) Using Local and Density Fitting Approximations. *J. Chem. Phys.* **2003**, *118*, 8149−8160.

(53) Schütz, M.; Manby, F. R. Linear Scaling Local Coupled Cluster Theory with Density Fitting. Part I: 4-External Integrals. *Phys. Chem. Chem. Phys.* **2003**, *5*, 3349.

(54) Werner, H.-J.; Schütz, M. An Efficient Local Coupled Cluster Method for Accurate Thermochemistry of Large Systems. *J. Chem. Phys.* **2011**, *135*, 144116.

(55) Beebe, N. H. F.; Linderberg, J. Simplifications in The Generation and Transformation of Two-Electron Integrals in Molecular Calculations. *Int. J. Quantum Chem.* **1977**, *12*, 683−705.

(56) Røeggen, I.; Wisløff-Nilssen, E. On the Beebe-Linderberg Two-Electron Integral Approximation. *Chem. Phys. Lett.* **1986**, *132*, 154−160.

(57) Koch, H.; de Meras, A. S.; Pedersen, T. B. Reduced Scaling in Electronic Structure Calculations Using Cholesky Decompositions. *J. Chem. Phys.* **2003**, *118*, 9481−9484.

(58) Aquilante, F.; Pedersen, T. B.; Lindh, R. Low-Cost Evaluation of The Exchange Fock Matrix from Cholesky and Density Fitting Representations of The Electron Repulsion Integrals. *J. Chem. Phys.* **2007**, *126*, 194106.

(59) DePrince, A. E.; Sherrill, C. D. Accuracy and Efficiency of Coupled-Cluster Theory Using Density Fitting/Cholesky Decomposition, Frozen Natural Orbitals, and a t1-Transformed Hamiltonian. *J. Chem. Theory Comput.* **2013**, *9*, 2687−2696.

(60) Bozkaya, U. Orbital-Optimized Second-Order Perturbation Theory with Density-Fitting and Cholesky Decomposition Approximations: An Efficient Implementation. *J. Chem. Theory Comput.* **2014**, *10*, 2371−2378.

(61) Bozkaya, U. Derivation of General Analytic Gradient Expressions for Density-Fitted Post-Hartree-Fock Methods: An Efficient Implementation for the Density-Fitted Second-Order Møller−Plesset Perturbation Theory. *J. Chem. Phys.* **2014**, *141*, 124108.

(62) Bozkaya, U. Analytic Energy Gradients and Spin Multiplicities for Orbital-Optimized Second-Order Perturbation Theory with Density-Fitting Approximation: An Efficient Implementation. *J. Chem. Theory Comput.* **2014**, *10*, 4389−4399.

(63) Bozkaya, U. Orbital-Optimized MP3 and MP2.5 with Density-Fitting and Cholesky Decomposition Approximations. *J. Chem. Theory Comput.* **2016**, *12*, 1179−1188.

(64) Bozkaya, U. Orbital-Optimized Linearized Coupled-Cluster Doubles with Density-Fitting and Cholesky Decomposition Approximations: An Efficient Implementation. *Phys. Chem. Chem. Phys.* **2016**, *18*, 11362−11373.

(65) Bozkaya, U.; Sherrill, C. D. Analytic Energy Gradients for the Coupled-Cluster Singles and Doubles Method with the Density-Fitting Approximation. *J. Chem. Phys.* **2016**, *144*, 174103.

(66) Bozkaya, U. A Noniterative Asymmetric Triple Excitation Correction for The Density-Fitted Coupled-Cluster Singles and Doubles Method: Preliminary Applications. *J. Chem. Phys.* **2016**, *144*, 144108.

(67) Bozkaya, U.; Sherrill, C. D. Analytic Energy Gradients for The Coupled-Cluster Singles and Doubles with Perturbative Triples Method with the Density-Fitting Approximation. *J. Chem. Phys.* **2017**, *147*, 044104−044114.

(68) Bozkaya, U. Analytic Energy Gradients for Orbital-Optimized MP3 and MP2.5 with the Density-Fitting Approximation: An Efficient Implementation. *J. Comput. Chem.* **2018**, *39*, 351−360.

(69) Bozkaya, U.; Ünal, A.; Alagöz, Y. Energy and Analytic Gradients for the Orbital-Optimized Coupled-Cluster Doubles Method with the Density-Fitting Approximation: An Efficient Implementation. *J. Chem. Phys.* **2020**, *153*, 244115.

(70) Alagöz, Y.; Ünal, A.; Bozkaya, U. Efficient Implementations of the Symmetric and Asymmetric Triple Excitation Corrections for the Orbital-Optimized Coupled-Cluster Doubles Method with the Density-Fitting Approximation. *J. Chem. Phys.* **2021**, *155*, 114104.

(71) Bozkaya, U.; Ermiş, B.; Alagöz, Y.; Ünal, A.; Uyar, A. K. MacroQC 1.0: An Electronic Structure Theory Software for Large-Scale Applications. *J. Chem. Phys.* **2022**, *156*, 044801.

(72) Shao, Y.; Gan, Z.; Epifanovsky, E.; Gilbert, A. T.; Wormit, M.; Kussmann, J.; Lange, A. W.; Behn, A.; Deng, J.; Feng, X.; Ghosh, D.; Goldey, M.; Horn, P. R.; Jacobson, L. D.; Kaliman, I.; Khaliullin, R. Z.; Kuś, T.; Landau, A.; Liu, J.; Proynov, E. I.; Rhee, Y. M.; Richard, R. M.; Rohrdanz, M. A.; Steele, R. P.; Sundstrom, E. J.; Woodcock, H. L.; Zimmerman, P. M.; Zuev, D.; Albrecht, B.; Alguire, E.; Austin, B.; Beran, G. J. O.; Bernard, Y. A.; Berquist, E.; Brandhorst, K.; Bravaya, K. B.; Brown, S. T.; Casanova, D.; Chang, C.-M.; Chen, Y.; Chien, S. H.; Closser, K. D.; Crittenden, D. L.; Diedenhofen, M.; DiStasio, R. A.; Do, H.; Dutoi, A. D.; Edgar, R. G.; Fatehi, S.; Fusti-Molnar, L.; Ghysels, A.; Golubeva-Zadorozhnaya, A.; Gomes, J.; Hanson-Heine, M. W.; Harbach, P. H.; Hauser, A. W.; Hohenstein, E. G.; Holden, Z. C.; Jagau, T.-C.; Ji, H.; Kaduk, B.; Khistyaev, K.; Kim, J.; Kim, J.; King, R. A.; Klunzinger, P.; Kosenkov, D.; Kowalczyk, T.; Krauter, C. M.; Lao, K. U.; Laurent, A. D.; Lawler, K. V.; Levchenko, S. V.; Lin, C. Y.; Liu, F.; Livshits, E.; Lochan, R. C.; Luenser, A.; Manohar, P.; Manzer, S. F.; Mao, S.-P.; Mardirossian, N.; Marenich, A. V.; Maurer, S. A.; Mayhall, N. J.; Neuscamman, E.; Oana, C. M.; Olivares-Amaya, R.; O'Neill, D. P.; Parkhill, J. A.; Perrine, T. M.; Peverati, R.; Prociuk, A.; Rehn, D. R.; Rosta, E.; Russ, N. J.; Sharada, S. M.; Sharma, S.; Small, D. W.; Sodt, A.; Stein, T.; Stück, D.; Su, Y.-C.; Thom, A. J.; Tsuchimochi, T.; Vanovschi, V.; Vogt, L.; Vydrov, O.; Wang, T.; Watson, M. A.; Wenzel, J.; White, A.; Williams, C. F.; Yang, J.; Yeganeh, S.; Yost, S. R.; You, Z.-Q.; Zhang, I. Y.; Zhang, X.; Zhao, Y.; Brooks, B. R.; Chan, G. K.; Chipman, D. M.; Cramer, C. J.; Goddard, W. A.; Gordon, M. S.; Hehre, W. J.; Klamt, A.; Schaefer, H. F.; Schmidt, M. W.; Sherrill, C. D.; Truhlar, D. G.; Warshel, A.; Xu, X.; Aspuru-Guzik, A.; Baer, R.; Bell, A. T.; Besley, N. A.; Chai, J.-D.; Dreuw, A.; Dunietz, B. D.; Furlani, T. R.; Gwaltney, S. R.; Hsu, C.-P.; Jung, Y.; Kong, J.; Lambrecht, D. S.; Liang, W.; Ochsenfeld, C.; Rassolov, V. A.; Slipchenko, L. V.; Subotnik, J. E.; Voorhis, T. V.; Herbert, J. M.; Krylov, A. I.; Gill, P. M.; Head-Gordon, M. Advances in Molecular Quantum Chemistry Contained in the Q-Chem 4 Program Package. *Mol. Phys.* **2015**, *113*, 184−215.

(73) Shavitt, I.; Bartlett, R. J. *Many-Body Methods in Chemistry and Physics*, 1st ed.; Cambridge Press: New York, 2009; pp 443−449.

(74) Davidson, E. R. The Iterative Calculation of a Few of the Lowest Eigenvalues and Corresponding Eigenvectors of Large Real-Symmetric Matrices. *J. Comput. Phys.* **1975**, *17*, 87−94.

(75) Liu, B. In *Numerical Algorithms in Chemistry: Algebraic Methods*; Moler, C., Shavitt, I., Eds.; Technical Report LBL-8158, Lawrence Berkeley Laboratory, University of California: Berkeley, 1978; pp 49−53.

(76) Sherrill, C. D.; Schaefer, H. F. The Configuration Interaction Method: Advances in Highly Correlated Approaches. *Adv. Quantum Chem.* **1999**, *34*, 143−269.

(77) Leininger, M. L.; Sherrill, C. D.; Allen, W. D.; Schaefer, H. F. Systematic Study of Selected Diagonalization Methods for Configuration Interaction Matrices. *J. Comput. Chem.* **2001**, *22*, 1574−1589.

(78) Saebø, S.; Pulay, P. Fourth-Order Møller−Plessett Perturbation Theory in The Local Correlation Treatment. I. Method. *J. Chem. Phys.* **1987**, *86*, 914.

(79) Scuseria, G. E.; Janssen, C. L.; Schaefer, H. F. An Efficient Reformulation of the Closed-Shell Coupled Cluster Single and Double Excitation (CCSD) Equations. *J. Chem. Phys.* **1988**, *89*, 7382−7387.

(80) Epifanovsky, E.; Zuev, D.; Feng, X.; Khistyaev, K.; Shao, Y.; Krylov, A. I. General Implementation of the Resolution-of-the-Identity and Cholesky Representations of Electron Repulsion Integrals within Coupled-Cluster and Equation-of-Motion Methods: Theory and Benchmarks. *J. Chem. Phys.* **2013**, *139*, 134105.

(81) Dunning, T. H. Gaussian Basis Sets for Use in Correlated Molecular Calculations. I. The Atoms Boron Through Neon and Hydrogen. *J. Chem. Phys.* **1989**, *90*, 1007−1023.

(82) Woon, D. E.; Dunning, T. H. Gaussian Basis Sets for Use in Correlated Molecular Calculations. V. Core-Valence Basis Sets for Boron through Neon. *J. Chem. Phys.* **1995**, *103*, 4572−4585.

(83) Weigend, F.; Köhn, A.; Hättig, C. Efficient Use of the Correlation Consistent Basis Sets in Resolution of the Identity MP2 Calculations. *J. Chem. Phys.* **2002**, *116*, 3175−3183.

(84) Manohar, P. U.; Krylov, A. I. A Noniterative Perturbative Triples Correction for the Spin-Flipping and Spin-Conserving Equation-of-Motion Coupled-Cluster Methods with Single and Double Substitutions. *J. Chem. Phys.* **2008**, *129*, 194105.